

Inelastic electron–dipole-molecule scattering at sub-milli-electron-volt energies: HF and NH₃

X. Ling, M. T. Frey, K. A. Smith, and F. B. Dunning

Department of Space Physics and Astronomy and the Rice Quantum Institute, Rice University, P.O. Box 1892, Houston, Texas 77251

(Received 17 February 1993)

Studies of destruction of very-high- n ($100 < n < 400$) Rydberg atoms in collisions with the polar targets HF and NH₃ are reported. Analysis of the data using the essentially-free-electron model suggests that, for ultralow electron energies ($\sim 80 \mu\text{eV}$ – 1.4 meV), the cross section $\sigma(\epsilon)$ for rotationally inelastic scattering of electrons by a polar target varies approximately as $1/\epsilon$, where ϵ is the electron energy.

PACS number(s): 34.80.−i, 34.60.+z

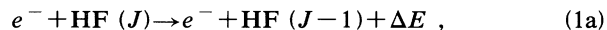
INTRODUCTION

Collisions involving Rydberg atoms are frequently described using the essentially-free-electron model in which it is assumed that the separation between the excited Rydberg electron and its associated core ion is so large that they behave as independent particles during all or part of the collision [1]. This model has been particularly effective in describing Rydberg-atom collisions with polar molecules and with targets that attach free low-energy electrons. Analysis of Rydberg-atom data has provided cross sections for free-electron attachment to a variety of molecules at subthermal electron energies and has illuminated the threshold behavior of such cross sections [2,3]. Measurements involving polar target molecules and Rydberg atoms with values of principal quantum number n up to $n \sim 40$ have demonstrated a number of effects that can be attributed to rotational energy transfer in a binary Rydberg-electron–target interaction [4–6]. In the present work we have extended the study of Rydberg-atom collisions with simple polar targets to very large values of n , $100 \leq n \leq 400$. In this range of n use of the essentially-free-electron model should be particularly well justified because the mean de Broglie wavelength of the Rydberg electron ($\lambda = h/p$, where p is the mean electron momentum) scales as n , whereas the mean atomic diameter scales as n^2 . Thus, as n increases, the electron is localized to a smaller fraction of the atomic volume and should behave increasingly as a free particle. For example, as n varies between 100 and 400 the mean kinetic energy of the Rydberg electron varies between $\sim 1.4 \text{ meV}$ and $80 \mu\text{eV}$. The corresponding de Broglie wavelengths range from ~ 330 to 1300 \AA and are much smaller than the associated atomic diameters ($2n^2a_0$, where a_0 is the Bohr radius), which vary between $\sim 10\,000$ and $160\,000 \text{ \AA}$. Thus it is reasonable to view the Rydberg electron as an essentially free particle and analysis of Rydberg atom collisions data can provide information on electron–polar-molecule scattering at energies extending into the μeV regime which has not been explored previously.

In this energy regime one might anticipate new collision physics. The de Broglie wavelength of the electron is somewhat larger than the range of the electron–target

interaction; the duration of the electron–target interaction is comparable to the rotational periods of most molecules; the distance between the core ion and target molecule changes significantly during one orbital period of the Rydberg electron ($1.6 \times 10^{-16} n^3 \text{ sec}$) and, in the case of rotationally inelastic collisions, the energy transferred to the electron is significantly larger than its initial energy.

The objective of the present work is to study rotationally inelastic electron–polar-molecule scattering at sub-milli-electron-volt collision energies. Earlier work at lower n has shown that Rydberg-atom collisions with rotating polar molecules are dominated by the binary interaction between the Rydberg electron and the target molecule [4–6]. In this interaction, molecular rotational energy can be transferred to the electron, either ionizing the atom or producing states of different n . Here we study collisions with HF and NH₃, which were selected because they are relatively simple rotors and because, at high n , all rotational-to-electronic energy transfers will lead to ionization. [The rotational constants for HF and NH₃, $B = 20.95$ and 9.44 cm^{-1} , respectively, are such that the energy released by the lowest-energy dipole-allowed rotational transition ($J = 1$ to $J = 0$) is sufficient to ionize Rydberg atoms with $n > 53$ for HF and $n > 78$ for NH₃.] Thus measurements of rate constants for collisional ionization can provide information on rotationally inelastic electron–polar-molecule scattering, i.e., on the reactions



Analysis of the data shows that, at ultralow electron energies, the cross section $\sigma_e(\epsilon)$ for rotationally inelastic electron–polar-molecule scattering varies approximately as $1/\epsilon$, where ϵ is the electron energy. This behavior is similar to that noted in earlier very-high- n studies using the more complex rotors CH₃I and CH₂Br₂ [7]. The interpretation of these earlier data was, however, complicated by the fact that both targets attach free low-energy electrons (HF and NH₃ do not) and that, at the lower values of n , not all rotational transitions necessarily lead to ionization.

EXPERIMENTAL METHOD

The present apparatus is shown schematically in Fig. 1 and has been described in detail elsewhere [2,7]. Briefly, potassium atoms contained in a thermal-energy (600-K) beam are photoexcited to a selected np state using a frequency-doubled Coherent CR699-21 Rh6G dye laser. The output of the laser is formed into a series of pulses of $\sim 2 \mu\text{sec}$ duration with a pulse repetition frequency of $\sim 5\text{--}10 \text{ kHz}$ using an acousto-optic modulator. Excitation occurs, in zero electric field and (typically) in the presence of target gas, near the center of an interaction region defined by three pairs of planar copper electrodes. Following excitation, collisions are allowed to occur for a predetermined time whereupon the number and excited-state distribution of Rydberg atoms remaining in the interaction region are determined using field ionization. A voltage ramp is applied to the lower electrode and the electrons resulting from field ionization are detected by a Johnston multiplier. In practice, the probability that a Rydberg atom is excited during any laser pulse is small, $\lesssim 0.02$, and the time development of the Rydberg-atom population is determined by accumulating data following many laser pulses.

Rydberg-atom collisions with polar targets lead to parent-state depopulation through state changing and ionization. The Rydberg-atom population in the interaction region thus comprises both parent np states and the products of state-changing reactions which, as will be justified below, can be treated as a single "mixed" population. Assuming that collisional ionization is the only process contributing to Rydberg-atom destruction, the time evolution of the parent and mixed populations $N_0(t)$ and $N_1(t)$, respectively, following any laser pulse, will be described by the rate equations

$$\frac{dN_0(t)}{dt} = -\rho(k_l + k_{i0})N_0(t) = -\rho k_d N_0(t), \quad (2)$$

$$\frac{dN_1(t)}{dt} = -\rho k_{i1}N_1(t) + \rho k_l N_0(t), \quad (3)$$

where t is the time after the end of the laser pulse, ρ is the target-gas number density (measured using an ionization gauge calibrated against a capacitance manometer), k_l is

the rate constant for state changing, and k_{i0} and k_{i1} are the rate constants for collisional ionization of parent atoms and the mixed population, respectively. $k_d (=k_l + k_{i0})$ is the rate constant for parent np state depopulation. (Effects due to spontaneous decay and background radiation can be neglected.) Solution of these equations yields

$$N_0(t) = N_0(0)e^{-\rho k_d t}, \quad (4)$$

$$N_1(t) = N_0(0) \frac{k_l}{k_d - k_{i1}} [e^{-\rho k_{i1} t} - e^{-\rho k_d t}] + N_1(0)e^{-\rho k_{i1} t}. \quad (5)$$

The time development of the total Rydberg-atom population $N(t)$ in the interaction region is thus given by

$$\begin{aligned} N(t) &= N_0(t) + N_1(t) \\ &= N_0(0) \left\{ \left[1 - \frac{k_l}{k_d - k_{i1}} \right] e^{-\rho k_d t} \right. \\ &\quad \left. + \left[\frac{k_l}{k_d - k_{i1}} + \frac{N_1(0)}{N_0(0)} \right] e^{-\rho k_{i1} t} \right\}. \quad (6) \end{aligned}$$

Because the evolution of the total Rydberg-atom population $N(t)$ is governed by three separate rate constants, care must be exercised in extracting rate constants from measurements of $N(t)$.

Information on parent-state depopulation and state changing, i.e., k_d and k_l , can be obtained by measuring the evolution of the Rydberg-atom population distribution in the interaction region using selective field ionization (SFI) in which the electron signal resulting from field ionization is measured as a function of applied field [4,6]. Since atoms in different states ionize at different field strengths, analysis of SFI data can provide information on the distribution of excited states present at the time of application of the SFI voltage ramp. SFI data pertaining to $\text{K}(150p)\text{-HF}$ and $\text{K}(150p)\text{-NH}_3$ collisions are presented in Fig. 2. These data were obtained using similar target-gas densities and collision times. Figure 2 also includes the range of field strength (inferred from earlier measurements [8]) over which diabatic and adiabatic ionization of atoms in states with $n \sim 150$ is expected. [Low (high) $|m_l|$ states tend to ionize adiabatically (diabatically).] SFI could not be used at values of $n \gtrsim 175$ because all states tended to ionize diabatically and it was not possible to separate parent and product states.

In the absence of target gas, the SFI spectrum comprises a single sharp peak that results from adiabatic ionization of the parent state. Collisions result in the growth of a broad, higher-field SFI feature. For HF, the high-field SFI feature can be attributed to diabatic ionization of atoms in states in n manifolds adjacent to the parent np state. Such states are nearly degenerate with the parent level and are populated, in essence, through elastic scattering of the Rydberg electron in its orbit by the target molecule. The width of the high-field SFI feature suggests that the products of such quasielastic state-changing reactions have a broad, possibly statisti-

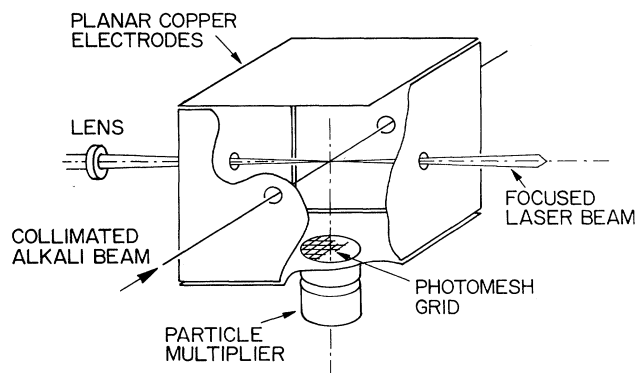


FIG. 1. Schematic diagram of the apparatus.

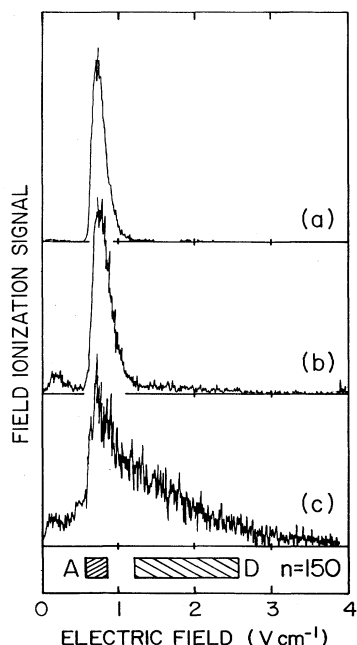


FIG. 2. SFI spectra pertaining to $K(150p)/HF, NH_3$ collisions. (a) SFI spectrum obtained with no target-gas present. (b) and (c) SFI spectra obtained after collisions with HF and NH_3 , respectively. These data were obtained using similar target-gas densities and collision times. To aid in comparison, all three SFI spectra are normalized to the same peak height. The horizontal bars beneath the data indicate the range of field strengths over which adiabatic (A) and diabatic (D) ionization of states with $n = 150$ is expected.

cal, distribution of l and $|m_l|$ values. The small peak at very low field strengths results primarily from electrons produced through collisional ionization that remain in the interaction region when the voltage ramp is applied. Ionization also occurs during the voltage ramp and produces a small background. No significant signal attributable to SFI was observed at field strengths characteristic of ionization of states with n much greater than 150, indicating that collisions populate states in, at most, a very restricted range of n manifolds adjacent to the parent level. Since single state-changing collisions lead directly to large changes in l and $|m_l|$, but not in n , it is reasonable to assume that, on average, subsequent collisions will not significantly alter the state-changed population distribution allowing the state-changed atoms to be considered as a single mixed population. Rate constants for parent state depopulation and for state changing were obtained by analysis of the time development of the parent and state-changed populations and are $k_d \sim 1.3 \times 10^{-6} \text{ cm}^3 \text{ sec}^{-1}$ and $k_l \sim 1 \times 10^{-7} \text{ cm}^3 \text{ sec}^{-1}$, respectively, at $n = 150$.

The SFI data indicate that, for HF, state-changing reactions are relatively unimportant, i.e., $N_1(t)$ is small. In addition, k_{i0} (which is approximately equal to k_d since k_l is small) is large and, as will be discussed, is expected to be substantially larger than k_{i1} . Thus Rydberg-atom de-

struction by HF is associated primarily with collisional ionization of parent np atoms. This can be seen by inspection of Eq. (6), which shows that for the present conditions, where $k_l/(k_d - k_{i1})$ and $N_1(0)/N_0(0)$ are small, the total Rydberg-atom population $N(t)$ will vary approximately as

$$N(t) \sim e^{-\rho k_d t} \equiv e^{-t/\tau_0}, \quad (7)$$

where $1/\tau_0 (\equiv \rho k_d \approx \rho k_{i0})$ is the destruction rate. Measurements confirmed that $N(t)$ was well described by a single exponential and that, as illustrated in Fig. 3(a), the destruction rate increased linearly with target-gas density ρ . Rate constants k_{i0} for collisional ionization of the parent np state derived from the pressure dependence of the destruction rates are presented in Fig. 4.

In the case of NH_3 the SFI feature corresponding to ionization of state-changed atoms is significantly larger than that observed with HF. This difference can be attributed partially to additional population of a localized group of states with $n \sim 164$ through near-resonant energy transfer involving transitions between NH_3 inversion levels [9]. Analysis of SFI data shows that the rate constant for state changing in collisions with NH_3 , $k_l \sim 2 \times 10^{-6} \text{ cm}^3 \text{ sec}^{-1}$ at $n = 150$, is very much larger than for HF. While inversion transitions must account, in part, for this difference, similarly large rate constants for state changing have been observed with a variety of other symmetric-top molecules having similar dipole moments [7]. The reason for the relatively small value of k_l for HF is not known, but it is reasonable to speculate that it might result because the molecular rotational period is comparable to the electron-molecule collision time. The dipole moment (which is aligned along the internuclear

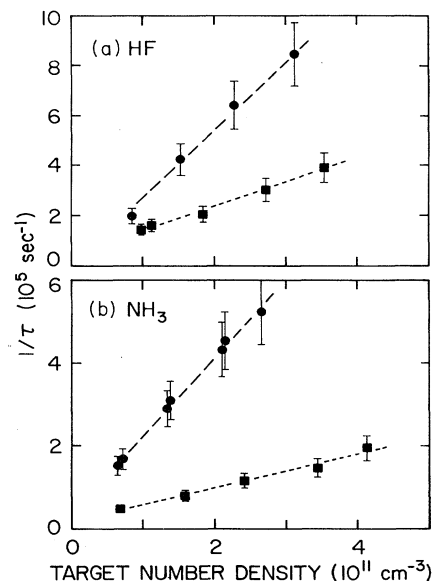


FIG. 3. Measured destruction rates $1/\tau$ as a function of target-gas density ρ for collisions with (a) HF and (b) NH_3 at $n = 100$ (\blacksquare) and $n = 300$ (\bullet).

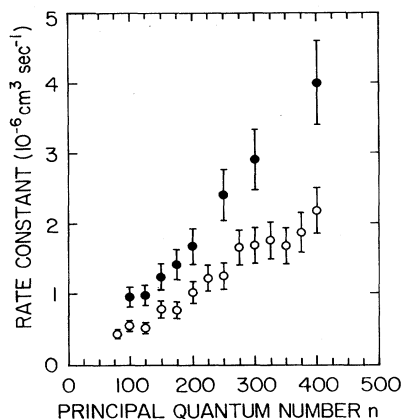


FIG. 4. ●, rate constants k_{i0} for ionization of $K(np)$ atoms in collisions with HF. ○, rate constants k_{i1} for ionization of a state-mixed population (see text) in collisions with NH_3

axis) will therefore tend to average to zero during the collision. In NH_3 , and other symmetric-top molecules, the dipole moment is aligned along the symmetry axis of the molecule. This axis, however, precesses about the total angular momentum, which is not usually parallel to the symmetry axis, and the component of the dipole moment parallel to the total angular momentum therefore does not average to zero and may be more effective in scattering the slowly moving electron. The SFI data also showed that the rate constant for parent-state depopulation in collisions with NH_3 is large, $k_d \sim 5 \times 10^{-6} \text{ cm}^3 \text{ sec}^{-1}$ at $n=150$. Although inversion transitions and quasielastic collisions can lead to small changes in n , these collisions still only populate states with a relatively narrow distribution of n near the parent value and it is again reasonable to consider the state-changed atoms as a single mixed population.

For NH_3 the rate constants for state changing are large, and it is not possible to accurately determine k_{i0} simply by measuring $N(t)$. However, for high target-gas densities and long collision times the number of state-changed atoms will greatly exceed the remaining parent-state population. In this limit, Rydberg-atom destruction is primarily associated with collisional ionization of state-changed atoms. This is also suggested by Eq. (6) because, as will be discussed, k_d is substantially larger than k_{i1} and for relatively large values of ρt the second term dominates when $N(t)$ evolves approximately as

$$N(t) \sim e^{-\rho k_{i1} t} \equiv e^{-t/\tau_1}, \quad (8)$$

where $1/\tau_1 (\equiv \rho k_{i1})$ is the destruction rate. Measurements confirmed that at high ρt values $N(t)$ was again well described by a single exponential and that, as shown in Fig. 3(b), the destruction rate increased linearly with target density. Rate constants k_{i1} for collisional ionization of the state-mixed population determined from the pressure dependence of the destruction rates are included in Fig. 4.

The data in Fig. 4 represent rate constants for

Rydberg-atom ionization in collisions with HF and NH_3 . It must be emphasized, however, that in the case of HF the data correspond to ionization of laser-excited np states, whereas for NH_3 the measurements are for ionization of a state-mixed population having a distribution of n and l values, although the range of n is quite small.

DISCUSSION

The linear increase observed in both k_{i0} (HF) and k_{i1} (NH_3) with n contrasts the behavior noted earlier in studies with the nonpolar attaching targets SF_6 and CCl_4 [2]. For these targets the rate constants for collisional ionization, which results primarily from capture of the Rydberg electron by the target molecule, are essentially independent of n over the present range. Such behavior is characteristic of an s -wave capture process and has been observed with a wide variety of attaching targets [3,10]. Electron capture is, however, fundamentally different from electron-polar-molecular scattering because it derives from a strong short-range interaction and because the product channel does not involve a free electron.

One possible explanation for the behavior evident in Fig. 4 is that as n increases, and the binding energy of the Rydberg electron decreases, the energy transfer associated with quasielastic scattering of the Rydberg electron by the target molecule becomes sufficient to lead directly to ionization. However, tests undertaken using CO_2 (electron- CO_2 scattering is characterized by an unusually large momentum-transfer cross section at low energies) failed to provide any evidence of such direct collisional ionization at $n=250$ and established an upper limit on the associated rate constant of $10^{-8} \text{ cm}^3 \text{ sec}^{-1}$. Further, if energy transfer accompanying quasielastic electron scattering led to significant collisional ionization, it would also be expected to populate a broad distribution of higher n states, and these are not observed in the SFI data.

The n dependence of the rate constants shown in Fig. 4 is therefore assumed to be associated with the characteristics of rotationally inelastic electron-polar-molecule scattering. According to the essentially-free-electron model, the rate constant for ionization through such rotational energy transfer should equal that for rotational deexcitation of the target molecule by free electrons having the same velocity distribution as the Rydberg electron, i.e.,

$$k_i = \int_0^\infty v \sigma_e(v) f(v) dv, \quad (9)$$

where $\sigma_e(v)$ is the cross section for rotationally inelastic scattering of free electrons with velocity v and $f(v)$ is the Rydberg-electron velocity distribution, which is determined by its quantum state. The observed linear increase in k_i with n suggests that $\sigma_e(v)$ varies approximately as $1/v^2$, i.e., as $1/\epsilon$. In this event Eq. (9) predicts that k_i should be proportional to $\langle 1/v \rangle$, which in turn is approximately proportional to n . The $1/v^2$ dependence for $\sigma_e(v)$ suggested by the data in Fig. 4 is consistent with the observation that, for NH_3 , the rate constant k_{i0} inferred for ionization of the parent $150p$ state is

significantly greater than that for ionization of l -mixed states of similar n . Specifically, the rate constant k_{i0} can be estimated using the relation $k_{i0} = k_d - k_l$, yielding the value $k_{i0} \sim 3 \times 10^{-6} \text{ cm}^3 \text{ sec}^{-1}$. Although this value is somewhat uncertain, it is still about four times larger than the value measured for ionization of a mixed population at $n = 150$. This difference can be rationalized by noting that, for a given n , $\langle 1/v \rangle$ for a p state is significantly larger than for a statistically mixed l distribution.

Expressions for $\sigma_e(v)$ have been derived using the Born approximation [see, for example, Eq. (9) in Ref. [11]] and suggest that for the present conditions, where the initial electron energy is very low and the final energy of the electron following scattering is substantially greater than its initial energy, $\sigma_e(v)$ should scale as $1/v$. Disagreement with the present data may not be particularly surprising, however, because the Born approximation assumes "weak" scattering, i.e., a small fractional change in the momentum of the scattered electron, and this is clearly not the case for the collisions considered here.

The present data are consistent with a simple "hard-sphere-electron" model, which assumes that reaction will always occur if the electron-molecule separation becomes on the order of the electron de Broglie wavelength. Such a model predicts a cross section that is proportional to the de Broglie wavelength squared, i.e., $1/v^2$ and yields the correct n dependence. In addition, the predicted cross sections are of the right order of magnitude. The model is, however, incomplete because the values of the present rate constants for ionization of an l -mixed popu-

lation by NH_3 are a factor of 3 smaller than those observed for a similarly mixed population in earlier studies with CH_2Br_2 [7], despite the fact that the dipole moments of these species are almost equal (1.43 and 1.47 D for CH_2Br_2 and NH_3 , respectively). This, coupled with the anomalously low rate constant for state changing observed with HF, indicates that the details of molecular rotation, including the rotational frequency and the distribution of spatial orientation states, may also play an important role in the electron-molecule interaction at ultralow electron energies. However, as discussed elsewhere [7], a complete analysis of electron-polar-molecule scattering should also include an examination of possible transient electronic states associated with the target dipole moment (1.82 D for HF) and of the influence of the target dipole potential in the exit channel.

The present work provides information on rotationally inelastic electron-dipole-molecular scattering at ultralow electron energies, well below those accessible using any alternate technique. The data indicate that the Born approximation does not adequately describe the scattering in the present regime, and new theoretical approaches must be considered.

ACKNOWLEDGMENTS

It is a pleasure to acknowledge valuable discussions with M. A. Morrison and D. W. Norcross during the course of this work. This research is supported by the National Science Foundation under Grant No. PHY-9113414 and by the Robert A. Welch Foundation.

-
- [1] For a discussion of the essentially-free-electron model see, for example, the articles by M. Matsuzawa and by A. P. Hickman, R. E. Olsen, and J. Pascale in *Rydberg States of Atoms and Molecules*, edited by R. F. Stebbings and F. B. Dunning (Cambridge University Press, New York, 1983).
- [2] X. Ling, B. G. Lindsay, K. A. Smith, and F. B. Dunning, *Phys. Rev. A* **45**, 242 (1992).
- [3] F. B. Dunning, *J. Phys. Chem.* **91**, 2244 (1987).
- [4] F. G. Kellert, K. A. Smith, R. D. Rundel, F. B. Dunning, and R. F. Stebbings, *J. Chem. Phys.* **72**, 3179 (1980); F. B. Dunning and R. F. Stebbings, *Annu. Rev. Phys. Chem.* **33**, 173 (1982).
- [5] A. Pesnelle, C. Ronge, M. Perdrix, and G. Watel, *Phys. Rev. A* **34**, 5146 (1986); **38**, 4560 (1988).
- [6] A. Kalamarides, L. N. Goeller, K. A. Smith, F. B. Dunning, M. Kimura, and N. F. Lane, *Phys. Rev. A* **36**, 3108 (1987).
- [7] X. Ling, K. A. Smith, and F. B. Dunning, *Phys. Rev. A* **47**, R1 (1993).
- [8] T. H. Jeys, G. B. McMillian, K. A. Smith, F. B. Dunning, and R. F. Stebbings, *Phys. Rev. A* **26**, 335 (1982).
- [9] X. Ling, M. T. Frey, K. A. Smith, and F. B. Dunning, *J. Chem. Phys.* **98**, 2486 (1993).
- [10] A. Chutjian and S. H. Alajajian, *Phys. Rev. A* **31**, 2885 (1985).
- [11] O. H. Crawford, *J. Chem. Phys.* **47**, 1100 (1967).